Journal of Engineering Technology

Volume 8, SI (Recent Trends in System Engineering), April 2019, PP. 90-107

RESEARCH ARTICLE -ENGINEERNG TECHNOLOGY

Modeling and Analyzing Through-Silicon Via (TSV) Noise Coupling Using Genetic Algorithms

Khaoula Ait Belaid [1], Hassan Belahrach[1,2], Hassan Ayad[1], Abdelilah Ghammaz[1]

[1] Laboratory of Electrical Systems and Telecommunications, Department of Physics, Faculty of Sciences and Technology, Cadi Ayyad University, Marrakesh, Morocco.
[2] Department of Electrical Engineering, Royal Air Academy (ERA), Marrakesh, Morocco.

Abstract: In this paper, an intelligent method which is genetic algorithms is used to model noise coupling in Three-Dimensional Integrated Circuit (3D-IC) based on TSVs. This technique is rarely used in this type of circuits. It allows computing all the elements of the noise model, which helps to estimate the noise transfer function in the frequency and time domain in 3D complicated systems. The noise models include TSVs, active circuits, and substrate. To validate the method, comparisons between the results found, measurements and 3D-TLM method are made. According to the obtained simulation and experimental results, it is found that the proposed method is valid, efficient and robust.

Keywords: 3D-IC, TSV-TSV coupling noise; TSV-Contact coupling noise; genetic algorithms, Electromagnetic Coupling.

1. Introduction

The IC technology evolution is motivated by the need to increase performance in addition to functionality, consequently reducing power and cost. To achieve this objective, several solutions have been used such as: scaling devices and associated interconnecting wire by implementing new materials [1,2,40], and founding enhancing architecture to reconfigure routing, hierarchy and building circuits [2,3,41]. The integration of different signals (digital, analog, RF) and technologies by increasing drive, introduces various design concepts for which planar (2D) technologies cannot be suitable. The conventional planar IC has limited establishment choices, and these limit system architecture performance improvements. This causes problems related to the interconnect loading in the network of long wires and the need for signal repeaters for clock distribution [2]. Thus, three-dimensional (3D) integrated circuit have been adopted. The 3D technology solves the problems related to interconnection delays, this technique makes it possible by reducing the gate delays and increasing interconnections using the short wires. These shorter wires decrease the average load capacitance and resistance and decrease the number of repeaters needed to regenerate signal on long wires. In addition, to enable integration of heterogeneous technologies, in the 3D design, a 2D chip is divided into several blocks, and each one is placed on a separate layer where each layer is stacked on top of each other. This may be exploited to build SoC by placing different circuits with performance requirements in different layers [4,5].

In 3D technology, the communication between stacked integrated circuits and devices requires vertical interconnections. The processing of vertical interconnections seems complicated compared to the planar one; indeed, having the electrical and mechanical characteristics could be very challenging. Several kinds of vertical interconnection have been proposed such as bonding wires, metal bumps, contactless communication in addition to Through-Silicon-Via (TSV) and a lot of them are popular in

the industry. To improve electrical performance, the TSV interconnections become the first choice to avoid using bonding wires and metal bumps.

The study of 3D architectures requires modeling the TSVs to extract equivalent circuits that describe the electrical characteristics of a specific interconnection structure. In relation to the topic, several papers have discussed the issue of modeling TSVs. In [6, 7], the authors proposed a methodology based on RF characterizations and simulations, leading to a frequency dependent analytical model including MOS effect of high ratio TSV. Others in [8], gave an efficient method to model TSV interconnections, this approach results in equivalent network parameters that include the combined effect of conductor, insulator and silicon substrate. Although the modeling method is based on solving Maxwell's equations in integral form, the method uses a small number of global modal basis functions and can be much faster than discretization-based and integral equation methods. In [9], an accurate electrical model of TSV considering metal-oxide-semiconductor (MOS) capacitance effects was proposed. Design guidelines were proposed for TSVs as variable capacitors. The MOS capacitance was accurately solving Poisson's equation in cylindrical coordinates. Other compact wide-band equivalent circuit model for electrical modeling of TSV has been presented in [10]. Rigorous closed-form formulas for the resistance and inductance of TSVs have been derived from the magneto-quasi-static theory with a Fourier-Bessel expansion approach, whereas analytical formulas from static solutions have been used to compute the capacitance and conductance. This equivalent circuit model can capture the important parasitic effects of TSVs including the skin effect, proximity effect, lossy effect of silicon, and semiconductor effect. Another different model of TSV in high frequency has been given in [11, 12]. This proposed model includes not only the TSV but also the bump and the redistribution layer (RDL), which are additional components when using TSVs for 3D-IC. The model is developed with analytic equations derived from the physical configuration. In other previous works [13], the RLC parameters of TSV were modeled as a function of physical parameters and material characteristics. The RLC model is applied to predict the resistance, inductance, and capacitance of small-geometry TSV architectures. The TSV impedance can also be extracted using a fully analytical and physical model and Green's function in high frequency [14].

A lot of previous works have given models of one TSV without considering general multi-TSV structures. The modeling of these structures and their time domain simulation is one of the important problems being studying in this domain. In complicated 3D structures, more signal TSVs are needed, so the TSV distribution density increases. Due to the highly dense distribution of TSVs, TSV noise coupling is expected to be a major concern for 3D-IC system design. Few papers have modeled the noise coupling problem in structures with several TSVs. In [36], the authors have described the equivalent-circuit model of differential TSV pair. The critical differential characteristics are analyzed and calculated in terms of the lumped-circuit model and the effective loop parameters of multi-TSVs. A novel π-type equivalent-circuit model of signal-ground TSV pairs considering eddy current and proximity effects is proposed in [37]. In [16], the authors have presented parasitic substrate coupling effects in 3D-IC due to TSVs. Electrical characterization is performed on dedicated test structures to extract electrical models of substrate coupling phenomena when RF signals. In [15, 12, and 38], a TSV noise coupling model is proposed based on a three-dimensional transmission line matrix method (3D-TLM). Using the proposed TSV noise coupling model, the noise transfer functions from TSV to TSV and TSV to the active circuit can be precisely estimated in complicated 3D structures.

In this paper, a TSV noise coupling model based on structures in [12, 15] and Genetic Algorithms (GA) is given. This work consists to compare the parameters to find by GA and those calculated using 3D-TLM and measurements of [12, 15]. By employing GAs, the 3D-substrate parameters can be computed at high frequencies. In additions, the models include most of the elements presented in actual circuits, such as redistribution layer (RDL) interconnects and substrate contact.

The rest of this paper is organized as follows. In section 2, first the noise coupling models in 3D-IC are described, then, genetic algorithms are applied to compute the element values of these models. The verification of the results and simulations are analyzed in section 3. The conclusions are drawn in the last section.

2. Modeling of TSV noise coupling using Genetic Algorithms

2.1 TSV-TSV and TSV-Active Circuit noise coupling

Noise coupling in 3D-IC based on TSV is a significant problem which causes serious effects. This type of noise degrades the circuit performance and makes system sensitivity dominated. It can also be transmitted directly to an active circuit through the substrate; therefore, the signal and power are corrupted, the system reliability is reduced, and the bit error rate is increased [17, 18]. A TSV is composed of a conductor surrounded by an insulation layer with a very small thickness which causes a high capacitance between the TSV and the substrate, as a consequence, high-frequency noise can be easily coupled from TSV to TSV or substrate and vice versa. In 3D-IC systems, more signal TSVs are used in a limited plane surface as illustrated in figure 1, which increases the distribution density of TSV. Because of this great density, the modeling of noise coupling between TSVs as well as TSV and the active circuit is an essential step of the design of these systems [19]. In this section, a TSV noise coupling model is given. The noise can be coupled through many paths: TSV to TSV or TSV to the substrate. For both paths, a model must be given.

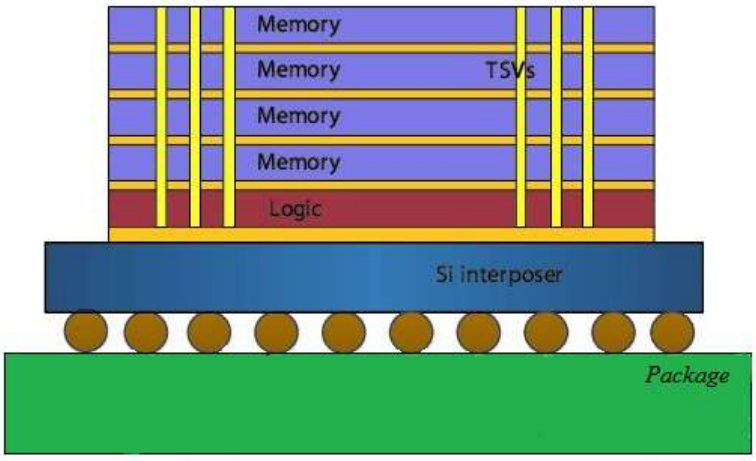

Figure. 1. 3D-IC using TSVs

The conceptual figure of TSV-to-TSV noise coupling is shown in figure 2. To model a circuit with several TSVs a basic structure had been adopted. This structure is composed of two signal TSVs, where one presents the aggressor and the other the victim, in addition to two ground TSVs connected using a ground line. Figure 3 shows the structure described. The previous structure can be modeled as an equivalent RLGC circuit based on the geometry and material properties. The RLGC circuit consists of a simple TSV's equivalent model, the RDL's model, and the substrate's model. The TSV model is composed of a capacitance C_{TSV} that represents the insulation layer surrounding the TSV. This capacitance can be derived from the coaxial-cable capacitance model since the TSV is filled with metal and the substrate is conductive; as well as a resistance R_{TSV} representing the material loss and the inductance which considers both the self-inductance $L_{TSV\text{-}self}$ and the mutual inductance $L_{TSV\text{-}mutual}$. The elements of the TSV model are given by the equations below.

$$C_{TSV} = \varepsilon_{oxTSV} \times \frac{2\pi h_{TSV}}{\ln\left(\frac{r_{TSV} + t_{oxTSV}}{r_{TSV}}\right)} \quad [F] \tag{1}$$

$$R_{TSV} = \frac{1}{\sigma_{TSV}} \times \sqrt{\left(\frac{h_{TSV}}{\pi r_{TSV}^2}\right)^2 + \left(\frac{h_{sub}}{\pi\left(r_{TSV}^2 - (r_{TSV} - \delta_{SKIN})^2\right)}\right)^2} \quad [\Omega] \tag{2}$$

$$\delta_{SKIN,depth} = \frac{1}{\sqrt{\pi f \mu \sigma_{TSV}}} \quad [m] \tag{3}$$

$$L_{TSV-self} = \frac{\mu h_{TSV}}{4\pi} \times \left[\ln\left(\frac{h_{TSV}}{r_{TSV}} + \sqrt{\left(\frac{h_{TSV}}{r_{TSV}}\right)^2 + 1}\right) + \frac{r_{TSV}}{h_{TSV}} - \sqrt{\left(\frac{r_{TSV}}{h_{TSV}}\right)^2 + 1}\right] \quad [H] \tag{4}$$

$$L_{TSV-mutual} = \frac{\mu h_{TSV}}{4\pi} \times \left[\ln\left(\frac{h_{TSV}}{p_{TSV}} + \sqrt{\left(\frac{h_{TSV}}{p_{TSV}}\right)^2 + 1}\right) + \frac{p_{TSV}}{h_{TSV}} - \sqrt{\left(\frac{p_{TSV}}{h_{TSV}}\right)^2 + 1}\right] \quad [H] \tag{5}$$

Where: h_{TSV} is the TSV height, r_{TSV} is the TSV radius, t_{oxTSV} is the oxide thickness, p_{TSV} is the pitch between TSVs, σ_{TSV} is the TSV conductivity, ε_{oxTSV} is the oxide permittivity, μ is the magnetic permeability, and δ is the skin depth dependent on material characteristics and on the frequency f.

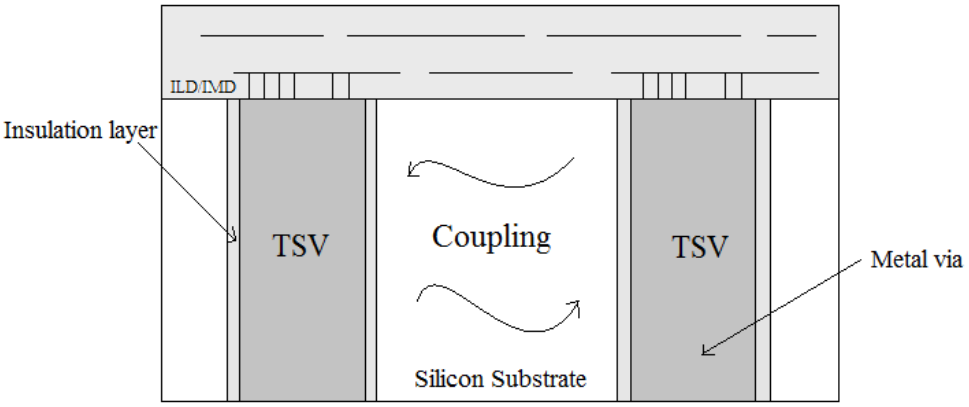

Figure. 2. A conceptual view of TSV-TSV noise coupling

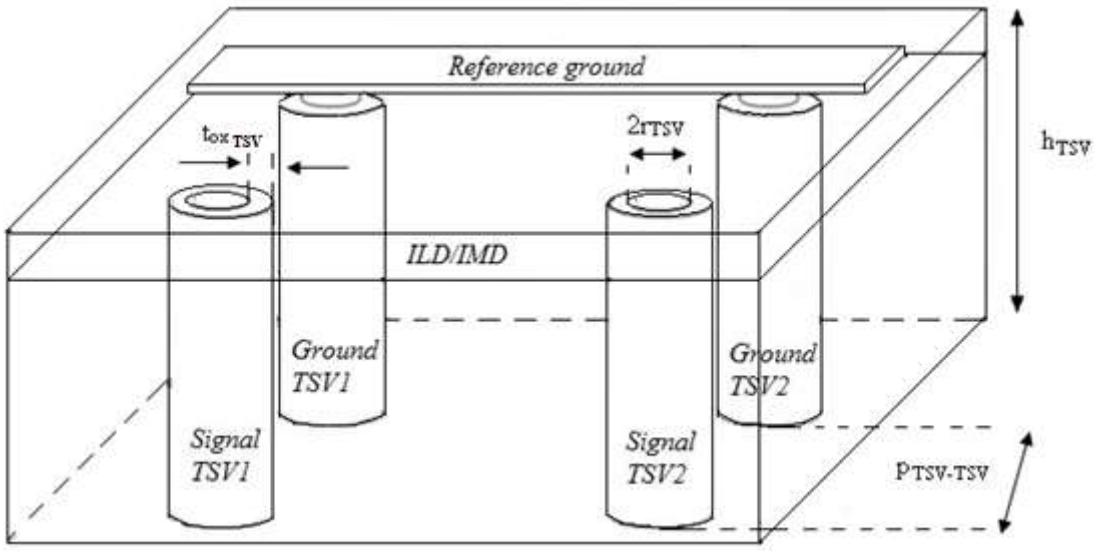

Figure. 3. Structure of the TSV-TSV coupling noise

Because of its distributed nature, the substrate cannot be translated into a compact analytic model accounting the entire chip area whose global effects are felt everywhere in the chip [20, 21]. In most cases, the substrate coupling models can be extracted from full 3-D numerical simulations using lumped-element models or a discretization of simplified form of Maxwell's equations [39,41]. The box integration formulation [22,23] can also help to find a distributed RC network. In this technique, a 3-D rectangular RC mesh network is constructed as an equivalent circuit representation of the modeled substrate. Based on this technique, the equivalent circuit model of the TSV-TSV coupling is given in figure 4. The equivalent circuit is composed of $C_{TSVtotal}$, which is the sum of C_{TSV} and C_{RDL}. In addition to five resistances and five capacitance which represent the substrate among the TSVs; and L_{gnd} the inductance of the metal connection between ground TSVs. In this equivalent circuit, the inductive coupling is negligible because the bottom side of the TSV is open. The TSV resistance does not influence the TSV-TSV noise coupling and is also neglected in the model.

The lumped circuit in figure 4 can be simplified into the equivalent circuit model in figure 5 using the techniques mentioned in [22, 24]. This equivalent circuit contains only three elements: the total equivalent TSV capacitance, substrate resistance, and substrate capacitance. Calculating these parameters is a delicate task, indeed the authors in [15] used the 3D-TLM method to do so. This technique can be used if a transmission line has a length smaller than the target wavelength. Using the 3D-TLM, the entire TSV coupling test structures are divided into several unit cells of TSV, a silicon substrate, substrate contact, and metal/RDL. Each unit cell is modeled using lumped R, C, L, and G elements, and the entire TSV noise coupling model is then constructed by combining these unit cell models in an appropriate manner. In the above-mentioned reference [15]; method parameters as well as the formulas for determining the components of the circuit; had been discussed in detail before and after simplification.

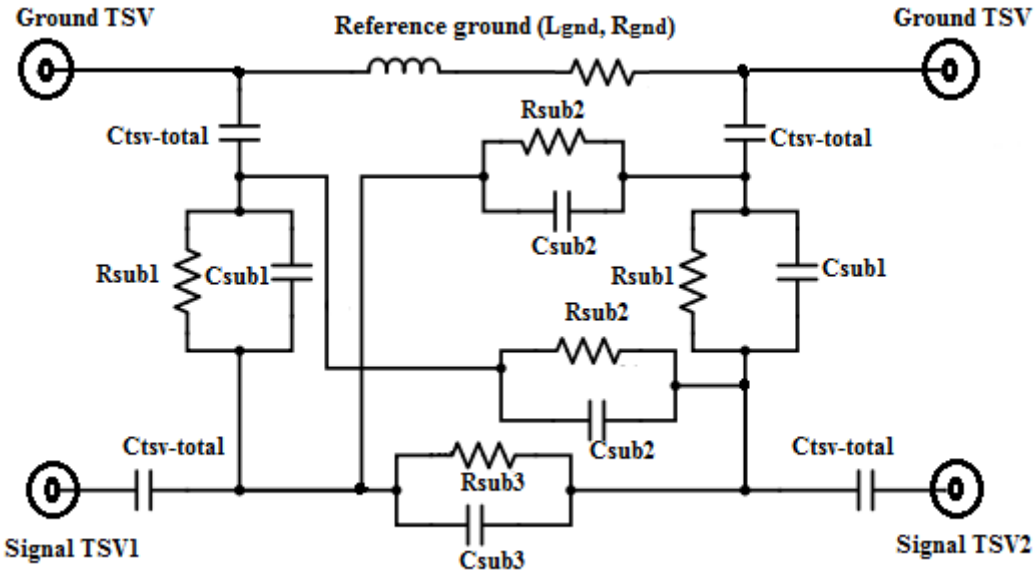

Figure. 4. The equivalent circuit model of TSV-TSV noise coupling

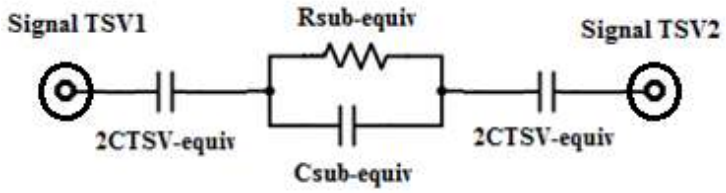

Figure. 5. A simplified model of the TSV-TSV noise coupling circuit

Since a 3D-ICs contains many silicon chips stacked by TSVs, and several MOSs are on these chips [29], the TSV-Active Circuit coupling must be modelized and analyzed. The conceptual view of this type of noise is depicted in figure 6. The structure in this figure is difficult to model because it includes many active circuits. Therefore, a simplification that considers a substrate contact instead of an active circuit was used. The P+ contact in a p-type silicon substrate can be represented as an active circuit, and the noise coupling between the TSV and the contact can be represented as the coupling between the TSV and the active circuit [15].

The test structure and the physical parameters of the TSV-contact noise coupling are presented in figure 7. The equivalent circuit model of this structure is illustrated in figure 8. Similar to the equivalent circuit of TSV-TSV noise coupling, the model is composed of $C_{TSVtoal}$; which is the sum of C_{TSV} and C_{RDL}; R_{sub} and C_{sub}, in addition to C_{ref} and L_{gnd} which represent the ground line parameters. The lumped circuit model in figure 8 can be simplified into the total equivalent circuit model in figure 9, which contains only three elements: the total equivalent TSV capacitance ($C_{TSV\text{-}equiv}$), the substrate resistance ($R_{sub\text{-}equiv}$), and the substrate capacitance ($C_{sub\text{-}equiv}$). In the case of TSV-Active circuit, it is difficult to propose equations to compute substrate resistance and capacitance values. Therefore, the authors in [15] used the 3D-LTM technique as explained before and, in this work, genetic algorithms were adopted to optimally search these values.

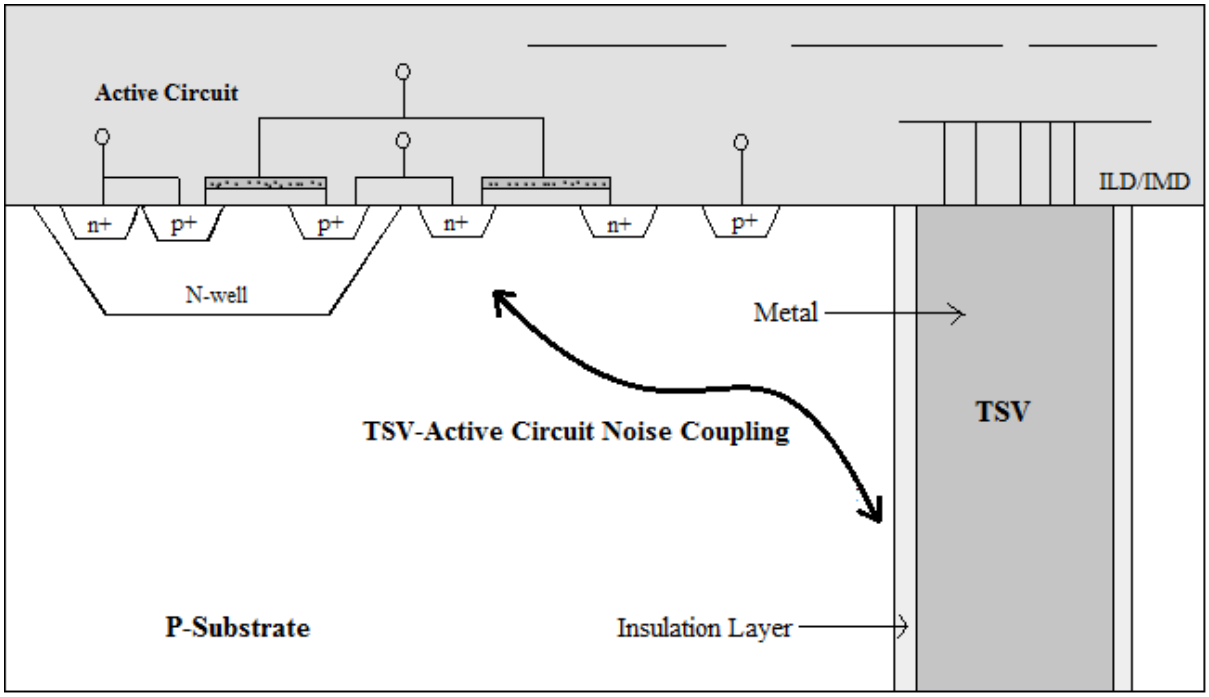

Figure. 6. The conceptual view of TSV-active circuit noise coupling

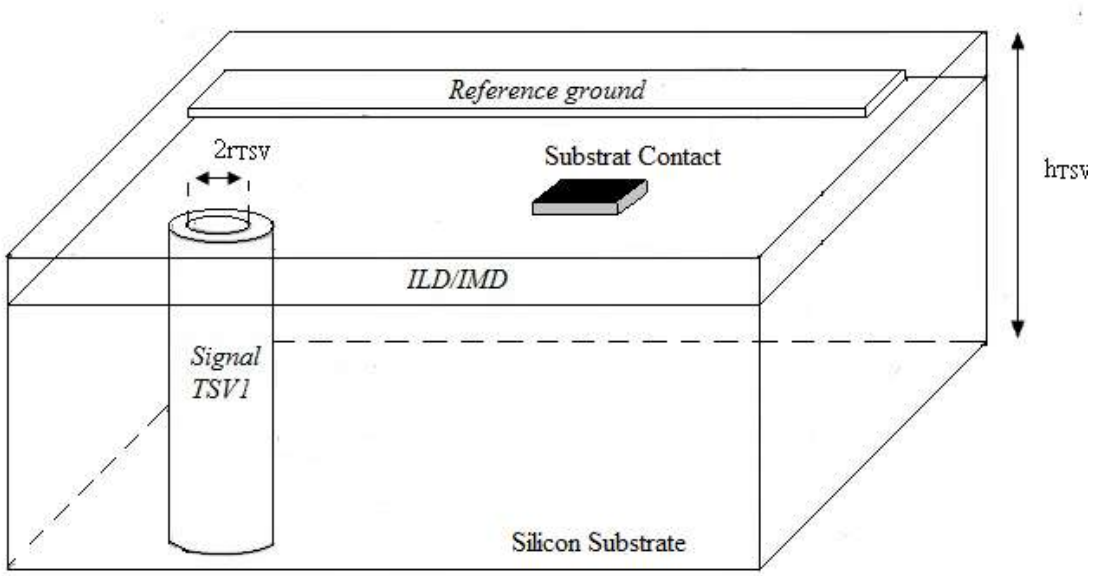

Figure. 7. Structure of the TSV-Active circuit noise coupling

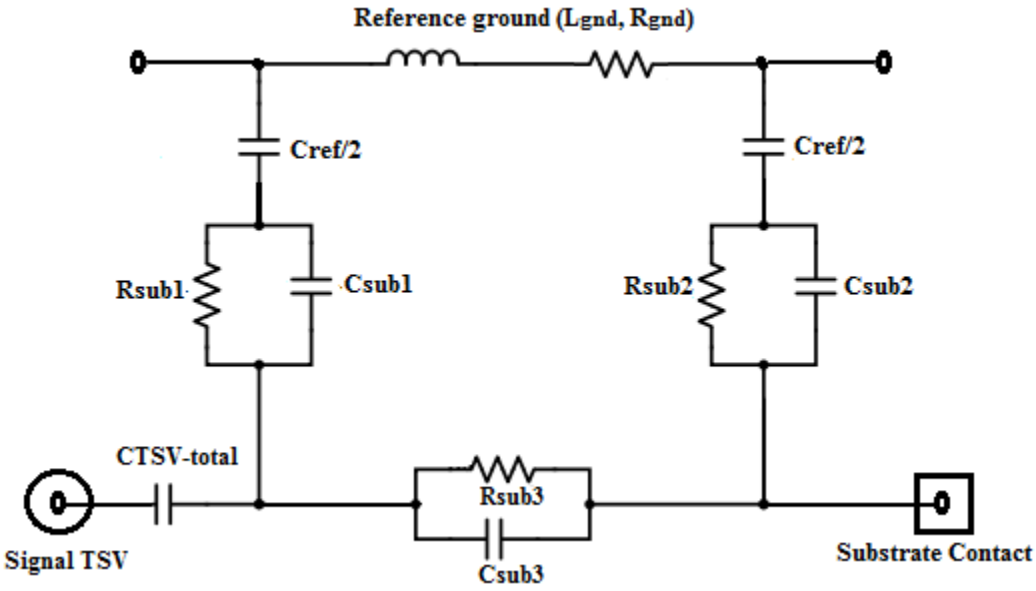

Figure.8. The equivalent circuit model of TSV-Active circuit noise coupling

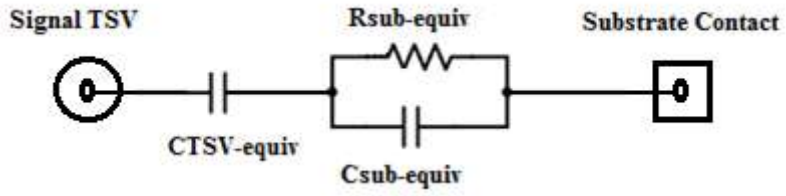

Figure.9. A simplified model of TSV-Active circuit noise coupling circuit

2.2 Genetic Algorithms Principle

The objective of this study was to calculate the parameters of the simplified circuit presented in figures 5 and 9, using an intelligent method called genetic algorithms.

Genetic algorithms are search algorithms based on the mechanics of natural genetics. They combine the survival of fittest among string structures with a structured yet randomized information exchange to form a search algorithm with some of the innovative flairs of human search. In every generation, a new set of artificial creatures is created using bits and pieces of the fittest of the old; an occasional new part is tried for good measure [25]. Genetic algorithms use a cost function based on a performance criterion to calculate a "fitness quality". The strongest individuals will be able to reproduce and have more descendants than the others. Each chromosome consists of a set of elements called characteristics or genes. The goal is to find the optimal combination of these elements that gives maximum fitness [25,26,27,28]. At each iteration (population generation), a new population is created from the previous population. There are many ways to proceed, genetic algorithms adapt to the problem studied.

There are several applications for genetic algorithms: optimization of difficult numerical functions, image processing, optimization of schedules, and industrial systems control [31,32,33]. They can also be used to optimize networks [34], and to find model parameters from experimental measurements.

In the beginning, genetic algorithms have a population P(0) of individuals with diverse characteristics and whose strings represent potential solutions to the problem being treated. Thus, the characteristics of individuals are coded by fixed-size strings of characters and individuals have no knowledge of a possible model. At each stage, the best individuals are selected according to an objective function and some individuals mutate or reproduce. The process is repeated until the

termination condition. The Evaluation uses the objective function that depends on the problem and that must be minimized or maximized.

Genetic algorithms are optimization algorithms based on techniques derived from genetics and natural evolution. Classically, there are three operators used which are selection, crossover, and mutation. The correct adequacy of the coding principle and the operators in relation to the problem addressed determines the success or failure of genetic algorithms. Therefore, it is important to choose these parameters carefully. The following paragraph provides a description of genetic operators.

Selection aims to select a sub-population from a parent population and makes it possible to identify the best individuals and eliminate the bad ones. The most common method is the roulette wheel, which is proportional to individual fitness. The number of times that an individual will be selected is equal to its fitness divided by the average fitness of the total population as given by equation (6) [35]; where P_j is the selection probability of each individual and S_i is the fitness function of the n^{th} individual. This function is decisive in a genetic algorithm and many much more complex selection methods are available: sigma scaling, Boltzman selection, and tournament selection.

$$P_j = \frac{S_j}{\sum_{k=0}^{n} S_k} \tag{6}$$

The first operator following the selection is the crossover. It consists of enriching the diversity of the population by manipulating chromosome's structures. Crossover considers two parents and generates two offspring. It consists of exchanging parents' genes in order to give offspring with combined properties. This exchange makes genetic algorithm efficient: sometimes, "good" genes from one parent replace the "bad" genes from another and create better-adapted solutions. The crossover can be done in several ways such as: one-point crossover, two points crossover, or barycentric crossover, in which two genes $P_1(i)$ and $P_2(i)$ are selected from each parent at the same position *i*, to create two new points $C_1(i)$ and $C_2(i)$ as presented by equation (7) [35]:

$$C_1(i) = (1-a)P_1(i) + aP_2(i) = aP_1(i) + (1-a)P_2(i)C_2(i) \tag{7}$$

Where *a* is a random weighting coefficient adapted to the definition's field of the gene.

The last operator is the mutation that occurs at fixed rates and it is a simple operator, flipping bits with a uniform distribution along the string. The objective is to prevent the genetic algorithm from converging towards local extremes of the function and to allow the creation of original elements. Several types of mutation can be used such as: uniform mutation; which evolves a parameter p_i ($b_{\inf} \le p_i \le b_{sub}$) chosen as part of the process into a randomly selected $p_i^{'}$ in the authorized domain, according to random number $a \in [0,1]$, as given by equation (8) [35]; non-uniform mutation, which has the particularity to remove the elements altered in a variable and small definition range. The mutation rate, in this case, can be computed using equation (9) [35], where: $a \in [-1,1]$, g the number of the current generation, G the full number of generations, $\alpha \prec 1$, and $\beta \succ 1$. In the end, genetic algorithms evaluate the individuals using fitness function and replace old individuals by new ones.

$$p_i^{'} = b_{\inf} + a(b_{\sup} - b_{\inf}) \tag{8}$$

$$p_i^{'} = \begin{cases} p_i + d\left(b_{\sup} - p_i\right) & si \quad d \succ 0 \\ p_i + d\left(p_i - b_{\inf}\right) & si \quad d \prec 0 \end{cases} \qquad avec \quad d = a.\exp\left[\left(\frac{g}{G}\right)^{\beta}.\ln(\alpha)\right] \tag{9}$$

Replacement operator is necessary for Genetic Algorithms. It defines the final individuals of the next generation. Two replacement types exist. The first is called elitist replacement, it consists in having a growing population size. In this type, the child is elected to be in the next just when it is at least better than the least successful of the parent generation. The second type, named a stationary replacement, keeps a constant population size. In this type, the best parents are kept for the next generation to maintain the population size.

The main steps of Genetic Algorithms could be summarized as the diagram presented in figure 10.

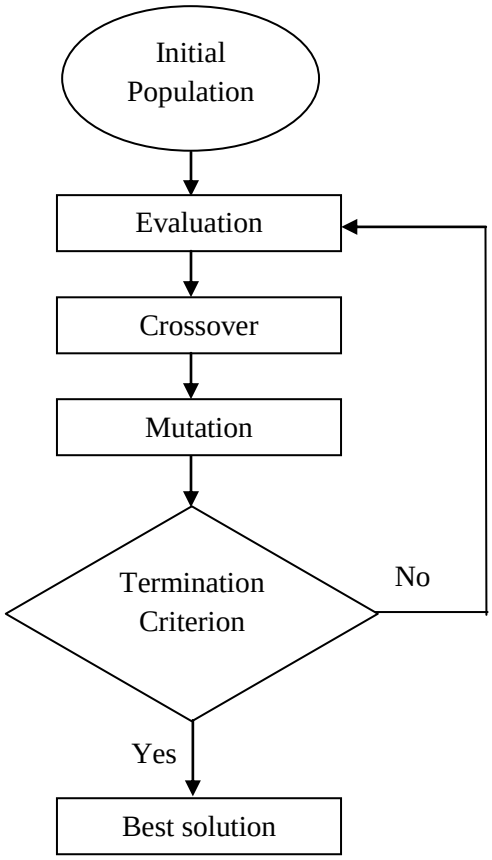

Figure. 10. The principal of Genetic Algorithms

For the optimization, each individual represents a point in the state space to which the value of the criterion to be optimized is associated. A random population of individuals is then generated for which the genetic algorithm focuses on selecting the best individuals while ensuring an efficient exploration of the state space. Genetic algorithms differ from classical optimization in four fundamental points: they seek a solution from a population of points and not from a single point, no regularity on the function studied is imposed, they are not determinist and use probabilistic transition rules, and no hypothesis of linearity or normality are used.

Our objective was to seek the parameters of the equivalent model of the TSV-TSV coupling as well as the TSV-Active Circuit coupling based on GAs and experimental measurements.

To perform this task, the following steps were done: first of all, the curve of experimental measurements which must be followed by the theory was drawn, then the transfer function of the

circuit according to unknown parameters, that are $C_{TSV\text{-}equiv}$, $R_{sub\text{-}equiv}$, and $C_{sub\text{-}equiv}$, was calculated, finally, genetic algorithms tried to find these parameters by making several iterations until the two curves were pasted together. For these algorithms to work properly, mutation, crossover, selection, and fitness function parameters must all be chosen correctly. In our problem, the fitness function was defined as the square of the difference between the experimental curve and the theoretically calculated transfer function. In fact, genetic algorithms optimized requested parameters by minimizing this error.

For TSV-Active Circuit noise coupling, Genetic Algorithms had been used as explained for the first, just that the transfer function and the experimental curve changed.

3. Simulations and Results:

In this section, the proposed method (GA) is verified by frequency and time domain measurements published in [12, 15]. So, all measurement curves used in this work were taken from these last references. To take the measurements of TSV-TSV noise coupling and verify its model, the test vehicles in figure 3 and figure 7 were fabricated using the Hynix via-last TSV process, according to this process, the RDL effects are significant, cannot be neglected and presented by C_{RDL} added to C_{TSV}. Concerning the manufacturing process of TSV, the top of the TSV was caved in, which prevents direct probing on the TSV, and the RDL line was used for the probing pad. The TSV had no interconnection on the bottom side, and the vehicle was placed on an insulator to isolate the conductive silicon substrate from the environment. The effects of the insulator were neglected because of its low dielectric constant [12]. An analyzer (VNA) was used to take measurements from 10 Mhz to 20 GHz. Table 1 shows all physical dimensions and material properties of the test vehicle.

Table 1. Physical dimensions and material properties of the test vehicle

Component	Value	Component	Value	Component	Value
r_{TSV}	16.5 µm	σ_{sub}	10 S/m	$d_{TSV\text{-}TSV}$	130 µm
$t_{ox\text{-}TSV}$	0.52 µm	σ_{TSV}	5.8×10^{7} S/m	$p_{TSV\text{-}TSV}$	250 µm
h_{sub}	100 µm	$\varepsilon_{r,sub}$	11.9		

For adjusting genetic algorithms; which were used to calculate the circuit parameters of figures 5 and 9 in such a way that the circuit transfer function that depends on these parameters follows the measurements whatever in the frequency domain as well as the time domain; the parameters in Table 2 were used. These parameters had been chosen carefully to ensure that the algorithm is effective. The population size of each generation was fixed at 100 individuals. The individuals of the algorithm are the parameters to find. The mutation was Gaussian. 2-point crossover with a crossover probability of 0.5 was used. The idea behind multi-point crossover is that parts of the chromosome that contribute to the fit behavior of an individual may not be in adjacent substrings. Furthermore, the disruptive nature of multi-point crossover may result in a more robust search by encouraging exploration of the search space rather than early convergence to highly fit individuals [30]. The tournament selection with a tournament size of 10 was used to select the parents at each generation. In tournament selection, the individuals are chosen randomly from the population and the best individual from this group is selected as a parent. This is repeated until enough parents have been chosen to produce the required number of individuals for the next generation. The fitness function was the square of the error (the difference) between experimental measurements and the fitness function of the circuit. This function is computed at the end of each generation for several frequency points. The simulations performed in this work were done using Matlab tool.

Table 2. Genetic Algorithm's parameters

Selection	Mutation	Crossover Function	Crossover Fraction
Tournament	Gaussian	Crossover two points	0.5

The parameters found by Genetic Algorithms and 3D-TLM of [12,15] are given in table 3. The measured noise and the noise transfer function of TSV-TSV coupling using GA's parameters in addition to the noise transfer function with the parameters in [12,15] are illustrated in figure 11. The noise transfer function was calculated when both ports are terminated with 50 Ω resistance.

Table 3 . TSV-TSV noise coupling parameters using GA and 3D-TLM

Methods	$C_{TSV\text{-}equiv}$ (fF)	$R_{sub\text{-}equiv}$ (Ω)	$C_{sub\text{-}equiv}$ (fF)
GAs	192.375	835.13	16.94
3D-TLM	201.3	928.5	11.2

Based on the results reported in figure 11, the proposed method, measurements and 3D-TLM agree well despite the difference which appeared in the frequencies higher than 3 GHz. Therefore, the method verification based on the measurement is valid. By analyzing the element values of table 3, one can see that the values calculated by GAs are close to those given by 3D-TLM. Yet, GAs generate a curve closer to that of measurements in high frequencies. The difference between the curves can be explained by the fact that the models estimate the low noise transfer function at high frequencies, where even low capacities cannot be neglected, or by a change in the characteristics of the test vehicle or by measurement errors.

The TSV-TSV noise coupling is divided into 3 regions. In region 1; from 10 MHz to 1 GHz; the $C_{TSV\text{-}equivalent}$ is the principal contributing element since the equivalent TSV is larger than the equivalent substrate resistance. In region 2; from 1 GHz to 12 GHz; the noise transfer function is defined by $R_{sub\text{-}equiv}$ because it becomes larger than $C_{TSV\text{-}equiv}$ impedance and smaller than $C_{sub\text{-}equiv}$ impedance. In region 3; frequencies above 12 GHz; $R_{sub\text{-}equiv}$ is larger than $C_{TSV\text{-}equiv}$ impedance and $C_{sub\text{-}equiv}$ impedance so, the noise transfer function is given by $C_{sub\text{-}equiv}$. The more the frequency increases, the more the noise increases.

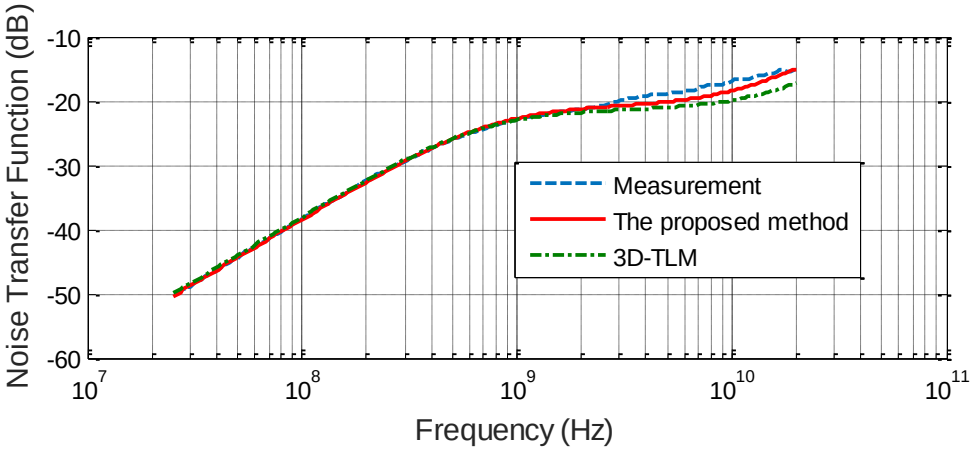

Figure.11. The proposed method, measured and 3D-TLM noise transfer function of TSV-TSV noise coupling

The proposed method in this work must also respect the transfer function in the time domain. Indeed, if the genetic algorithm finds parameters that correspond to the transfer function in the frequency domain but do not go with the time domain, the tests must be redone. The proposed and measurement method of the TSV-TSV noise coupling of the test vehicle in the time domain at frequencies 100 MHz and 1 GHz are illustrated respectively in figures 12 and 13. For temporal simulations, a trapezoidal signal switching from 0 to 1 V with a rising/falling time of 40 ps and source resistance of 50 Ω was used at port 1 and the coupling noise at port 2 was simulated using PSPICE

tool. According to figures 12 and 13, the method used to compute the parameters of figure 5 is verified and valid.

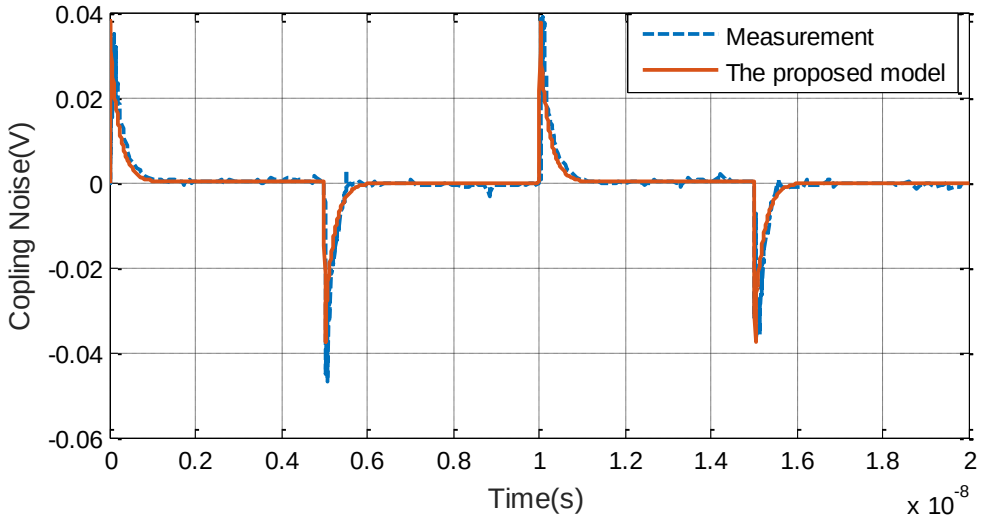

Figure.12. The proposed method and measured coupling of TSV-TSV test vehicle (the input clock frequency at port 1 is 100 MHz)

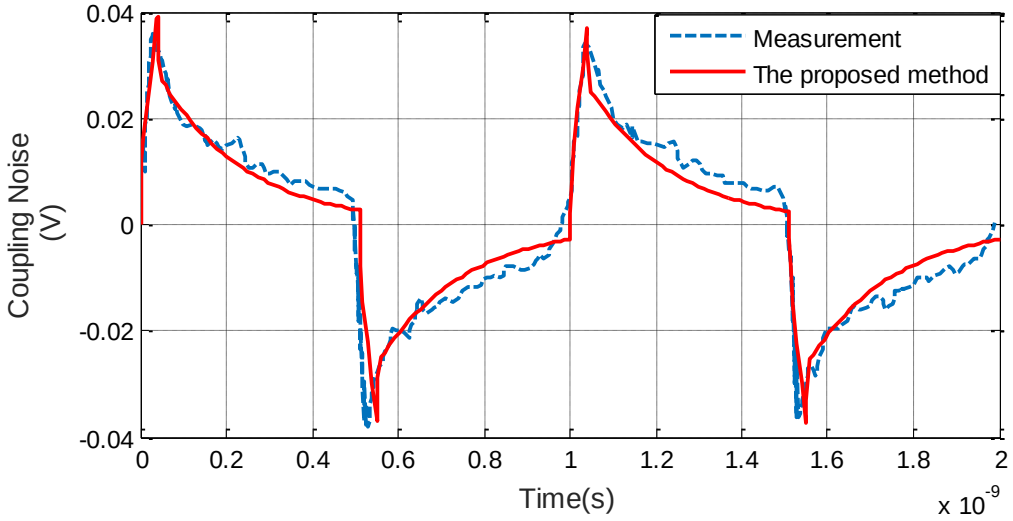

Figure.13. The proposed method and measured coupling of TSV-TSV test vehicle (the input clock frequency at port 1 is 1 GHz)

For the TSV-active circuit coupling model, by using GA, each lumped circuit value in figure 9 was obtained. All GA's parameters of the TSV-Contact coupling test vehicle are respectively presented in table 4. The population size of each GA's generation was fixed at 100 individuals. The mutation was defined as 0.2, 2-point crossover with a crossover probability of 0.4 was used, and the tournament selection with a tournament size of 10 was chosen. The fitness function stilled the square of the difference between experimental measurements and the transfer function of the circuit. Element values of the lumped circuit of TSV-contact coupling computed by the proposed method and 3D-TLM are presented in table 5.

Table 4. Genetic Algorithm's parameters

Selection	Mutation	Crossover Function	Crossover Fraction
Tournament	0.2	Crossover two points	0.4

Table 5. The TSV-contact noise coupling parameters using GA and 3D-TLM

Methods	$C_{TSV\text{-}equiv}$ (fF)	$R_{sub\text{-}equiv}$ (Ω)	$C_{sub\text{-}equiv}$ (fF)
GAs	815.21	870.74	14.08
3D-TLM	817.5	879.8	12

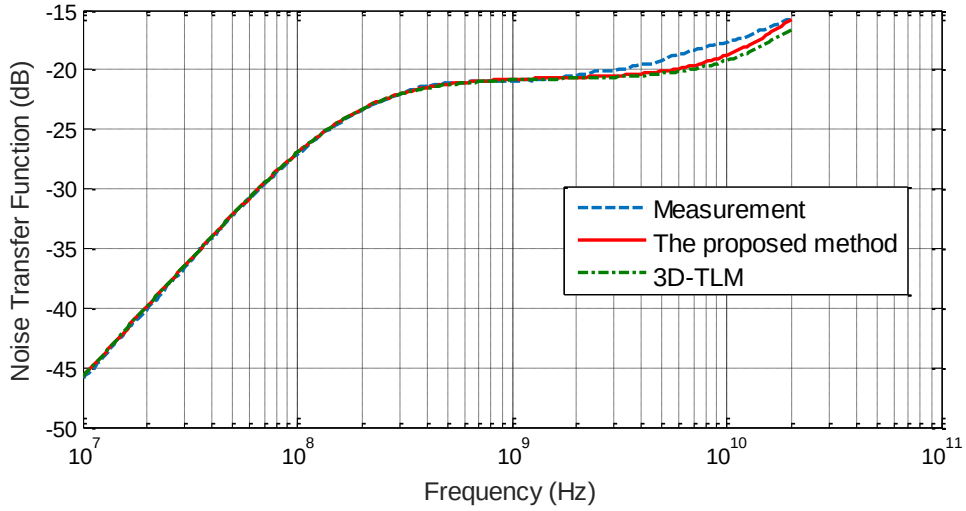

Figure 14. The proposed method, measured and 3D-TLM noise transfer function of TSV-Contact coupling

The measured, 3D-TLM and the proposed method for the TSV-contact coupling noise are illustrated in figure 13. Based on the results presented in this figure, the proposed method was closely matching the experimental results and 3D-TLM method. The proposed method verification based on the measurements was valid. Gas were more efficient than 3D-TLM method since the curve given by these algorithms is closer to the measurements than that given by 3D-TLM technique.

The TSV-contact noise coupling is identical to the TSV-TSV noise coupling. The transfer function is divided into three frequency behaviors regions, where each region is dominated by an element of the model in figure 9 as already explained above. In this case, as the frequency increases the noise increases, in addition, the noise is more important than the TSV-TSV case, this is due to the high value of $C_{TSV\text{-}equiv}$ of a single TSV.

The simulations in the time domain are presented in figures 16 and 17 respectively. These simulations were performed using the same characteristics cited for TSV-TSV noise. A trapezoidal signal switching from 0 to 1 V with a rising/falling time of 40 ps and source resistance of 50 Ω was used. The simulations were made in PSPICE tool at 100 MHz and 1 GHz.

By analyzing these results, one can see that the proposed method gave a behavior that reflects the experimental. Therefore, the proposed method was validated in the time-domain as well as the frequency-domain.

Observing figures 12-15, the peak-to-peak noise coupling in both studied cases is about 0.08 V. This value is already high and can even increase, therefore these noises should be considered.

Modeling 3D structures based on TSVs seems to be a very complicated task that needs to be taken into consideration. Many well-known analytical methods such as FDTD and 3D-TLM had been used to achieve the objective. These methods require a lot of calculation and time, but they are suitable.
This work had adopted an intelligent method (GA) that is rarely used in this field. Genetic algorithms are easy to use and do not require a lot of simulation time. All you must do is to adapt them to the studied problem and choose their parameters carefully.

The results found in this work, based on genetic algorithms, were conventional to experimental results. These results were even closer than those found by 3D-TLM used in [15]. It is true that both methods found similar results, but a small improvement validated by the experimental was noticed by the proposed method. The results proved that genetic algorithms are effective and robust.

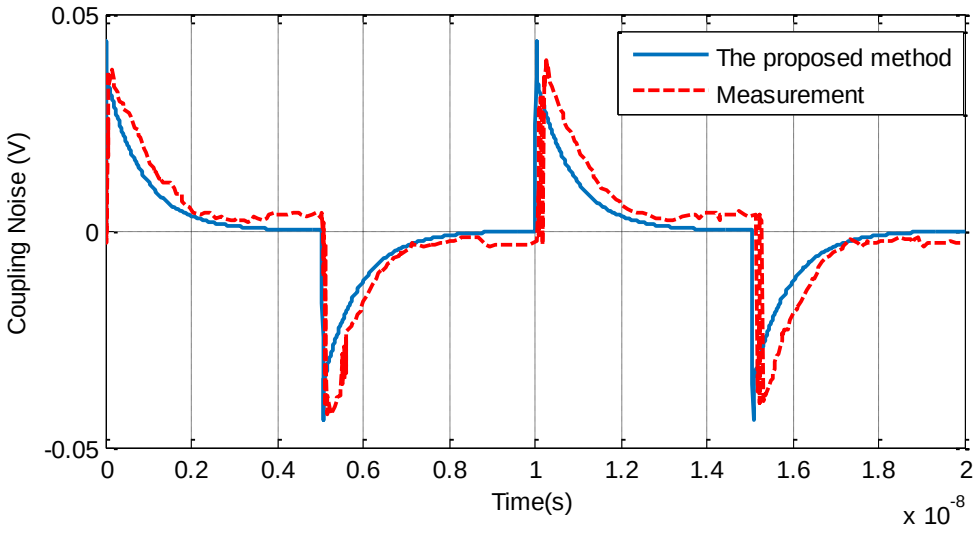

Figure.15. The proposed method and measured coupling noise of TSV-Contact test vehicle (the input clock frequency at port 1 is 100 Mhz)

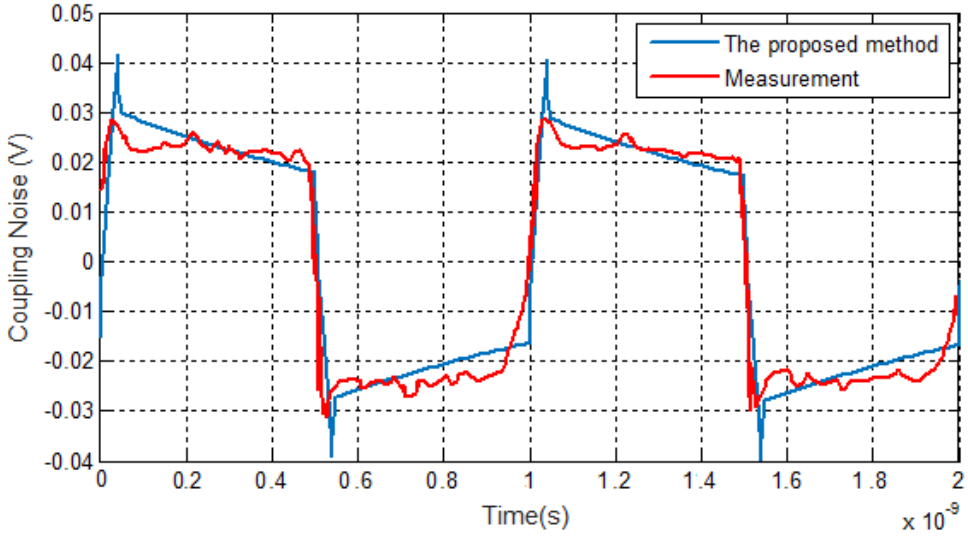

Figure. 16. The proposed method and measured coupling noise of TSV-Contact test vehicle (the input clock frequency at port 1 is 1 Ghz)

In this work, a complicated model with several TSVs (more than two) was presented, this model was replaced by another reduced model, which is similar to the coupling model between two TSVs but reflects the coupling behavior of several TSVs. From the found results, it can be concluded that any structure with several TSVs in the same level can be replaced by the simple model, it is just necessary to find a method to compute the parameters of the reduced circuit, and as already explained, genetic algorithms remain a good tool.

4. Conclusions

3-D integrated architecture based on TSVs is a relatively new research and widely used. Yet, these architectures have some difficulties mainly in their modeling and analysis. Accordingly, a new method to model them is necessary.

In this paper, genetic algorithms were proposed to compute the parameters of TSV-TSV and TSV-contact noise coupling in 3-D IC design. Both models included the equivalent circuit of the TSV, RDL, metal interconnects and the substrate. Indeed, the model can represent a practical 3D-IC system design. Using genetic algorithms, the parameters of previous models were found which substantiated to estimate the noise transfer function in three frequency regions from 10 MHz to 20 GHz.

To validate the proposed technique based on genetic algorithms, frequency and time measurements as well as the analytical method used on [15] were applied. Obtained results showed a good agreement between the proposed method and experiments. They also showed an improvement compared to 3D-TLM. These algorithms were easy to apply, did not require a lot of simulation time, efficient and robust.

References

[1]. Agarwal. V, Hrishikash. MS, Keckler. SW, and Burger. D, “Clock Rate Versus IPC: The End of the Road for Conventional Microarchitectures”, ACM SIGARCH Computer Architecture News 2000; 28(2):248-259.

[2]. Topol. AW, Tulipe. DC, Shi. Jr, Frank. DJ, Bernstein. K, Stein. SE, Kumar. A, Singco. GU, Young. AM, Guarini. KW, and Leong. M, “Three-Dimensional Integrated Circuits”, IBM J.RES. & DEV 2006; 50(415).

[3]. Salah. K, El Rouby. A, Ragai. H, and Ismail. Y, "3D/TSV Enabling Technologies for SOC/NOC: Modeling and Design Challenges", 22nd International Conference on Microelectronics 2010.
[4]. Siozios. K, Bartzas. A, and Soudris. D, "Architecture-Level Exploration of Alternative Interconnection Schemes Targeting 3D FPGAs: A Software-Supported Methodology", International Journal of Reconfigurable Computing 2008.
[5]. Kim. DH, Mukhopadhyay. S, and Lim. SK, "TSV aware Interconnect Length and Power Prediction for 3D Stacked ICs", IEEE International Interconnect Technology Conference 2009; 26-28.
[6]. Cadix. L, Fuchs. C, Rousseau. M, Leduc. H, and Chaabouni. H, "Integration and frequency dependent parametric modeling of Through Silicon Via involved in high density 3D chip stacking", ECS Transactions 2010; 33(12):1-21.
[7]. Ryu. C, Lee. J, Lee. H, Lee. H, Oh. T and Kim. J, "High Frequency Electrical Model of Through Wafer Via for 3D Stacked Chip Packaging", Proceedings of ESTC 2006; 215-220.
[8]. Han. KJ, Swaminathan. M, and Bandyopadhyay. T, "Electromagnetic Modeling of TSV Interconnections Using Cylindrical Modal Basis Function", IEEE Transactions on Advanced Packaging 2010; 33(4).
[9]. Bandyopadhyay. T, Han. KJ, Chung. D, Chatterjee. R, Swaminathan. M, and Tummala. M, "Rigorous Electrical Modeling of TSVs with MOS Capacitance Effects", IEEE Transactions on components, packaging and Manufacturing Technology 2011; 1(6).
[10]. Liu. EX, Li. EP, Ewe. WB, Lee. HM, and Gao. S, "Compact Wideband Equivalent Circuit Model for Electrical Modeling of TSV", IEEE Transactions on Microwave Theory and Techniques 2011; 59(6).
[11]. Kim. J, Pak. JS, Cho. J, Song. E, Lee. J, Park. K, Yang. S, Suh. M, and Byum. K, "High-Frequency Scalable Electrical Model and Analysis of TSV", IEEE Transaction Components Packaging and Manufacturing Technology 2011; 1(2):181-195.
[12]. Lee. M, Pak. JS, and Kim. J, "Electrical Design of Through Silicon Via", Springer Dordrecht Heidelberg New York London 2014.
[13]. Katti. G, Stucchi. M, Meyer. KD, and Dehaene. W, "Electrical Modeling and Characterization of TSV for 3-D ICs", IEEE Transactions on Electron Devices 2010; 57(1):256-262.
[14]. Xu. C, Kourkoulos. V, Suaya. R, and Banerjee. K, "A fully Analytical Model for the Series Impedance of TSV with Consideration of Substrate Effects and Coupling with Horizontal Interconnects", IEEE Transactions on Electron Devices 2011; 58(10):3529-3540.
[15]. Cho. J, Song. E, Yoon. K, Pak. JS, Kim. J, Lee. W, Song. T, Kim. K, Lee. J,Lee. H, Park. K, Yang. S, Such. M, Byun. K, and Kim. J, "Modeling and Analysis of TSV noise Coupling and Suppressing Using a Guard Ring", IEEE Transactions on Components, Packaging and Manufacturing Technology 2011; 1(2):220-233.
[16]. Eid. E, Lacrevaz. T, Bermond. C, Capraro. S, Roullard. J, Flechet. B, Cadix. L, Farcy. A, Ancey. P, Calmon. F, Valorge. O, and Leduc. P, "characterization and Modeling RF Substrate Coupling Effects Due to Vertical Interconnects in 3D Integrated Circuit Stacking", Elsevier Microelectronic Engineering 2011; 88:729-733.
[17]. Shim. Y, Park. J, Kim. J, Song. E, Yoo. J, Pak. JS, and Kim. J, "Modeling and analysis of simultaneous switching noise coupling for a CMOS negative-feedback operational amplifier in system-in-package", IEEE Trans. Electromagn. Compatibil 2009; 51(3):763–773.
[18]. Koo. K, Shim. Y, Yoon. C, Kim. J, Yoo. J, Pak. JS, and Kim. J, "Modeling and analysis of power supply noise imbalance on ultra-high frequency differential low noise amplifiers in a system-in-package", IEEE Trans. Adv. Packag. 2010; 33(3):602-616.
[19]. Han. K, "Electromagnetic Modeling of Interconnections in Three-Dimensional Integration", School of Electrical and Computer Engineering Georgia Institute of Technology 2009.
[20]. Afzali-Kusha. A, Nagata. K, Verghese. K, and Allstot. J, "Substrate Noise Coupling in SoC Design: Modeling, Avoidance, and Validation", Proceedings of the IEEE 2006; 94(12):2109-2138.
[21]. Nagata. M, Morie. T, and Iwata. A, "Modeling substrate noise generation in CMOS digital integrated circuits", in Proc. IEEE Custom Integrated Circuits Conf. 2002; 501-504.
[22]. Kerns. KJ, Wemple. IL, and Yang. AT, "Stable and efficient reduction of substrate model networks using congruence transforms", in Proc. IEEE/ACM Int. Conf. Computer-Aided Design 1995; 207-214.

[23]. Verghese. NK, Allstot. DJ, and Masui. S, "Rapid simulation of substrate coupling effects in mixed-mode ICs", in Proc. IEEE Custom Integrated Circuits Conf. 1993; 18.3.1-18.3.4.
[24]. Van Genderen. DJ, Van der Meijs. NP, "Reduced RC Models for IC Interconnections with Coupling Capacitances", IEEE Explorer 1992; 132-136.
[25]. Goldberg. D, "Genetic Algorithms in Search Optimization and Machine Learning", Reading Menlo Park: Addison Wesley, MA 1989; 412: 95-99.
[26]. Reed. P, Minsker. B, and Goldberg. D, "Designing a Competent simple genetic algorithm for search and optimization", Water Resources Research 2000; 36:3757-3761.
[27]. Nicoara. E, "Solving Scheduling in Pharmaceutical Industry with Genetic Algorithms", Journal of Control Engineering and Applied Informatics 2007; 9:19-26.
[28]. Baghli. L, "Contribution à la commande de la machine asynchrone, utilisation de la logique floue, des réseaux de neurones et des algorithmes génétiques", Point Carré University, Nancy, France 1999.

[29]. Dreiza. M, Yoshida. A, Micksch. J, and Smith. L, "Stacked Package-on-Package Design Guide", Chip Scale Review 2005.
[30]. Jong. KAD, Spears. WM, "A formal analysis of the role of multi-point crossover in genetic algorithms", Annals of Mathematics and Artificial Intelligence Journal 5 1992; 1-26.
[31]. Nordin. P, Keller. RE and Banzhaf. W, "Francone fd genetic programming: an introduction: On the automatic evolution of computer programs and its applications", Morgan Kaufmann 1998; 69:1236-1239.
[32]. Pictet. O, Zumbach. G, and Bhattacharyya. S, "Representational semantics for genetic programming-based learning in high-frequency financial data", Genetic Programming: Proc. 3rd Annual Conf. 1998;11-16.
[33]. Lopes. HS, Freitas. AA, and Bojarczuk. CC, "Discovering comprehensible classification rules using genetic programming: a case study in a medical domain", roc. Genetic and Evolutionary Computation Conference (GECCO-99), Orlando, FL, USA 1999; 953-958 :1236-1239.
[34]. Picarougne. F, "Recherche d'information sur internet par algorithmes évolutionnaires", Doctoral Thesis, Tours University, France, 2000.
[35]. Bouarifi. W, "Assimilation Variationnelle des conditions initiales par contrôle optimal et identification de paramètres par algorithmes génétiques dans le modèle ICARE", Doctoral Thesis, Cady Ayyad University, Morocco, 2009.
[36]. Qu. C, Ding. D, and Zhu. Z, "High-Frequency Electrical Modeling and Characterization of Differential TSVs for 3-D Integration Applications", IEEE Microwave and Wireless Components Letters 2017; 27(8):721-723.
[37]. Lu. Q, Zhu. Z, Yang. Y, Ding. R, and Li. Y, "High-Frequency Electrical Model of Through-Silicon Vias for 3-D Integrated Circuits Considering Eddy-Current and Proximity Effects", IEEE Trans. on Components, Packaging and Manufacturing Technology 2017; 7(12):2036-2044.
[38]. Lim.J et al., "Modeling and Analysis of TSV Noise Coupling Effects on RF LC-VCO and Shielding Structures in 3D IC", IEEE Transaction on Electromagnetic Compatibility 2018; 60(6):1939-1947.
[39]. Soleimanpour. R, and Kalantari. K, "Numerical Investigation of Drag Reduction Using Electromagnetic", Journal of Engineering Technology 2015; 3(2):158-173.
[40]. Mahmoudabadi. ND, Moghadam. BF, "Comparison of Shuffled Complex Evolution Algorithm and modified shuffled Frog Leaping Algorithm for Optimal Allocation and Sizing of Distributed Generation", Journal of Engineering Technology 2015; 3(2):174-185.
[41]. Bhattacharjee. P, Dey. A, Chakraborty. SK, and Geoswami. RS, "Implementation of Ternary Logic in QCA using SPICE Macro-Modeling", Journal of Engineering Technology 2016; 5(2):143-155.